PHYSICAL REVIEW A **89**, 021405(R) (2014)

Laser-induced breakup of helium ^3S $1s2s$ with intermediate doubly excited states

A. S. Simonsen,[1,*] H. Bachau,[2] and M. Førre[1,†]

[1]*Department of Physics and Technology, University of Bergen, N-5007 Bergen, Norway*

[2]*Centre des Lasers Intenses et Applications, CNRS-CEA-Université Bordeaux I, 33405 Talence Cedex, France*

(Received 11 July 2013; revised manuscript received 11 December 2013; published 26 February 2014)

Solving the time-dependent Schrödinger equation in full dimensionality for two electrons, it is found that in the XUV regime the two-photon double ionization dynamics of He($1s2s$) is predominantly dictated by the process of resonance enhanced multiphoton ionization via doubly excited states (DESs). We have studied a pump-probe scenario where the full laser-driven breakup of the ^3S $1s2s$ metastable state is dominated by intermediate quasiresonant excitation to doubly excited (autoionizing) states in the $^3P^o$ series. Clear evidence of multipath interference effects is revealed in the resulting angular distributions of the ejected electrons in cases where more than one intermediate DES is populated in the process.

DOI: 10.1103/PhysRevA.89.021405 PACS number(s): 32.80.Rm, 32.80.Zb, 42.50.Hz

The role of electron correlation has puzzled physicists since the early days of quantum mechanics, and it complicates dynamical processes to a degree that necessitates the forsaking of the independent particle picture. Due to advances in computer technology, studies investigating correlated electron dynamics are being performed in *ab initio* frameworks, solving correlated few-electron systems without approximations. On the experimental side, development of high-order harmonic generation (HHG) and free-electron laser (FEL) light sources makes it possible to meet the pulse characteristics required to study correlated few-photon fragmentation of the simplest two-electron systems. Here, the processes of one-photon double ionization and two-photon double ionization (TPDI) of helium are ideal benchmarks for probing electron correlation. In the last decade, the scenario of direct (nonsequential) TPDI of He($1s^2$) has received considerable attention, both theoretically [1–15] and experimentally [16–21]. More recently, the analogous process in H_2 [22–27] and H^- [28] was studied. The excited $^{1,3}S$ $1s2s$ states of He have received considerably less attention. Double ionization due to single-photon impact was investigated [29–32], while TPDI was studied for photon energies above the sequential threshold [33].

It is well established that the resonant excitation of doubly excited states (DESs) strongly influences the photoionization dynamics. As such, DESs are also expected to play a decisive role in two-photon double-ionization processes once such states are energetically accessible in the laser field. Therefore, knowledge of the role of DESs in multiphoton double-ionization processes is essential for uncovering the correlated dynamics of complex atoms and molecules exposed to state-of-the-art HHG and FEL fields. Here, the process of two-photon double ionization of He($1s2s$) provides an ideal benchmark for testing the impact of intermediate DESs. The singly excited $^{1,3}S$ $1s2s$ states of helium differ from the He($1s^2$) ground state in that DESs are present within the nonsequential regime for TPDI. The case of He($1s2s$) is also of general validity in view of current interest in double-ionization processes involving complex systems where the ionizing electrons originate from different orbitals. Considering, e.g., lithium, TPDI involves the absorption of two photons from an asymmetric configuration $1s2s$, a case that is currently under theoretical [34] and experimental [35] investigation. Laser-driven processes in helium which involve DESs have been studied previously, including probing electron correlations in highly excited autoionizing states [36], probing two-electron dynamics by double ionization [37], enhanced nonlinear double excitation from the ground state [38], and two-photon interferometry [39].

In this Rapid Communication, we explore the laser-driven two-photon complete breakup of the helium ^3S $1s2s$ metastable triplet state. We show that the TPDI occurs predominantly through intermediate excitation of the $^3P^o$ series of DESs, due to the process of resonance enhanced multiphoton ionization (REMPI). In order to isolate the signal pertaining to ionization of $^3P^o$ solely, a pump-probe scenario is studied, where the pump pulse photon energy equals the excitation energy of various $^3P^o$ DESs. It is shown that whenever two or more DESs are populated simultaneously in the excitation process, clear signatures of interference are exhibited in the correlated angular distributions of the photoelectrons in the double continuum.

We approach the problem by solving the time-dependent Schrödinger equation (TDSE) in full dimensionality for the two electrons, applying a time propagation scheme previously described in [11]. In short, we expand the two-electron wave function in a basis comprised of B splines [40,41] and spherical harmonics in the radial and angular coordinates, respectively. For the ^3S $1s2s$ initial state, we obtain the binding energy $E_b = 2.1752$ a.u. (59.190 eV). The discretized TDSE is solved in a two-electron radial box extending to 270 a.u. in a basis comprised of 105 coupled channels, including all angular momenta $l_1, l_2 \leqslant 12$. The computations have been carefully checked for convergence by varying the number of B splines and coupled channels included in the basis. The laser pulses comprise linearly polarized electric fields and we assume the validity of the dipole approximation while representing the interaction between the electrons and the fields in the velocity gauge. The pulses are assumed to be sine squared with peak intensity 10^{13} W/cm^2, which makes three-photon processes and depletion of the initial state negligible. The momentum-resolved sixfold differential probability distribution for the double continuum is extracted by projecting the final wave

*aleksander.simonsen@ift.uib.no

†morten.forre@ift.uib.no

function onto products of one-electron Coulomb waves. Even though electron correlations are taken into account throughout the propagation of the TDSE, the Coulomb wave projection technique here only represents an approximation to the full problem, in the sense that the electron-electron repulsion is omitted when separate electron observables $(E_1, E_2, \Omega_1, \Omega_2)$ are mapped to the two-electron wave function. Therefore, in order to diminish the effect of the electron-electron interaction in the final wave packet, and to assure convergence of our results, we propagate the wave function for some additional optical cycles after the conclusion of the laser pulse(s). The latter approach has been used in several investigations treating the TPDI of He($1s^2$) (see, for example, [8] which focuses on the convergence of the approach), and it is also efficient in our case as the electrons tend to be ejected into opposite half-planes, causing the interelectronic distance to increase rapidly with time for the double-ionized electrons.

In order to describe the intermediate states, we adopt the classification scheme used by Lin [42], where DES are classified according to the following approximate quantum numbers: $n(K,T)N^A$, N and n defining the principal quantum numbers of the inner and outer electrons, respectively. The K and T quantum numbers refer to angular correlation properties. For larger positive values of K the two electrons tend to stay on opposite sides of the nucleus, whereas if K is negative they are more on the same side. The value of T is related to the projection of the total angular momentum along the interelectronic axis, e.g., if $T = 0$ the electrons tend to orbit in the same plane [42]. Furthermore, A $(+1,0,-1)$ relates to radial correlations. The "±" designation emphasizes whether the electrons approach the nucleus out of phase (for "−" states) or in phase (for "+" states) [43], i.e., whether the two-electron wave function has a node $(-)$ or antinode $(+)$ at $r_1 = r_2$.

Figure 1 depicts the total two-photon double-ionization yield versus photon energy. The signature of the intermediate $2(1,0)2^+$ resonance of the $^3P^o$ series, which we shall call $2s2p$ for simplicity, is clearly expressed at the photon energy 38.5 eV. The $2s2p$ resonance is significantly populated in the excitation process. As such, the underlying ionization mechanism is an example of a REMPI process where the $2s2p$ plays the role of the intermediate state. This state, whose binding energy is $E_b = 20.7$ eV, is well separated from the other DESs in the $^3P^o$ series. The next group of states is located

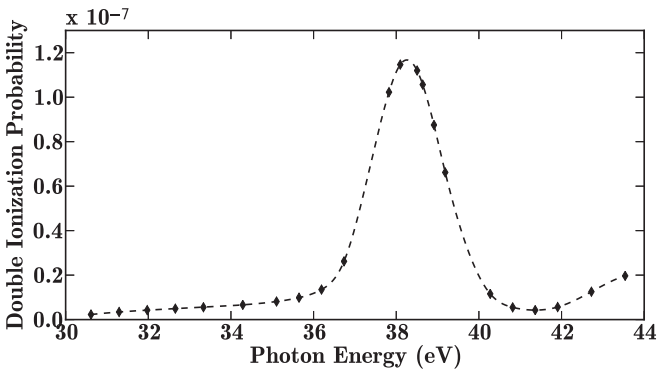

FIG. 1. The total two-photon double ionization yield as a function of photon energy for the process of two-photon double ionization by a single pulse of duration 40 cycles and peak intensity 10^{13} W/cm^2.

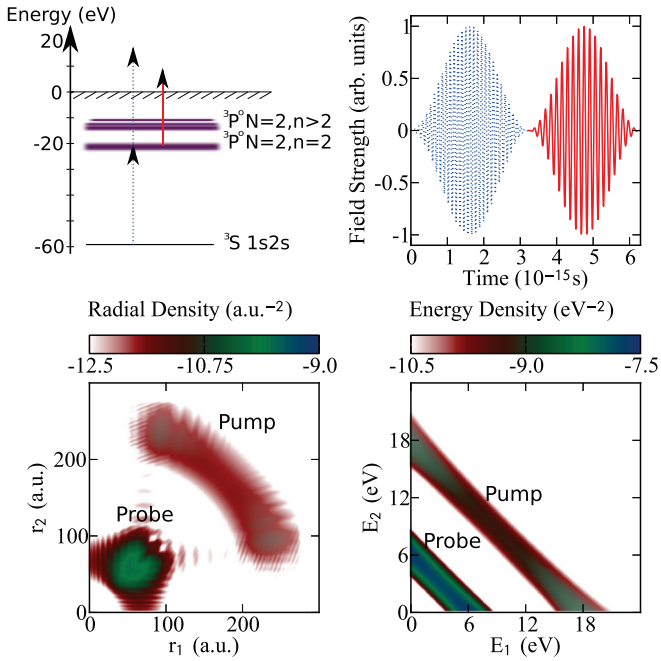

FIG. 2. (Color online) Schematic setup of the two-color pump-probe scheme. The blue arrows correspond to the primary (pump) laser pulse, whereas the red arrow pertains to transitions which involve absorption of a photon from the secondary (probe) pulse. The 30-cycle pump pulse is resonant with the excitation to $2s2p$ ($\hbar\omega = 38.5$ eV), whereas the probe pulse (20-cycle) has a driving frequency corresponding to $\hbar\omega = 27.2$ eV. In the top-right panel, the time evolution of the laser pulses is displayed. The two lower panels show the logarithm of the probability density for double ionization extracted five optical cycles after the conclusion of the probe pulse in both radial (left) and energy space (right).

at lower binding energies, i.e., at 15.9 eV and below [44]. Since the lifetimes of all these DESs are of the order of 100 fs and longer [44], and the duration of the laser pulses considered here is of the order of a few femtoseconds, the relevant autoionizing states remain quasistationary on this time scale, i.e., their decay into the adjacent $1skp$ single continuum plays a negligible role in the double-ionization process.

We will now demonstrate a general pump-probe scheme where one or more DESs in the $^3P^o$ series is first excited by the pump pulse. Then, at some time delay a probe pulse is applied in order to doubly ionize the resonance states. The setup is shown in Fig. 2 where the pump and probe pulses are depicted by dotted blue and solid red lines, respectively. Two pathways to the double continuum are illustrated (top-left panel), the first being two-photon capture during the pump pulse. The second pathway pertains to one-photon excitation, driven by the pump pulse, to a doubly excited state in the $^3P^o$ series, followed by double photoionization during the probe pulse. In the case illustrated in Fig. 2, the 30-cycle pump pulse has a driving frequency corresponding to $\hbar\omega = 38.5$ eV, making it resonant with the ^3S $1s2s$-^3P $2s2p$ transition, whereas for the 20-cycle probe pulse, $\hbar\omega = 27.2$ eV. The double-ionization yield is displayed in the lower-left panel of Fig. 2, represented as a radial-density plot (on logarithmic scale) of the doubly ionized wave packet. Notice the two contributions which are

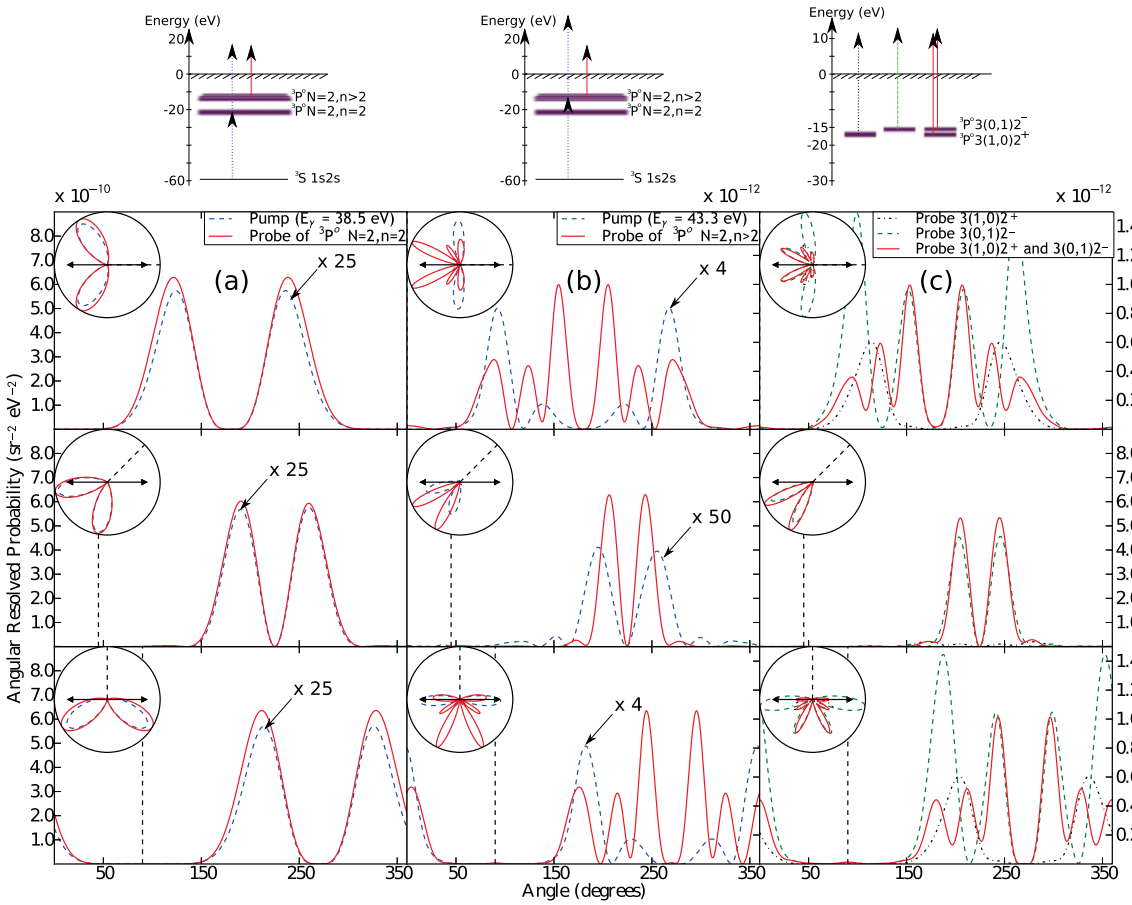

FIG. 3. (Color online) Double ionization probability distribution resolved in the ejection angle of electron two with respect to the polarization direction of the laser pulse, for the pump-probe scenario sketched in Fig. 2. The ejection angle of electron one is fixed at 0° (upper graph), 45° (center graph), and 90° (lower graph) with respect to the polarization direction. The distributions correspond to the two wave packets originating from the pump (dashed blue) and probe (solid red) (cf., lower left panel in Fig. 2). The vertical dashed lines define the prefixed escape direction of electron one, whereas the arrows in the polar plots indicate the direction of polarization. The angular distributions pertaining to the signal produced during the pump pulse have been scaled with the indicated factors for comparison. Left panel (a): Pump pulse photon energy $\hbar\omega = 38.5$ eV (dashed blue) and probe pulse photon energy $\hbar\omega = 27.2$ eV (solid red). Middle panel (b): Pump pulse photon energy $\hbar\omega = 43.3$ eV (dashed blue) and probe pulse photon energy $\hbar\omega = 27.2$ eV (solid red). Right panel (c): The relative contribution of $3(1,0)2^+$ (dotted black) and $3(0,1)2^-$ (dashed green) separately, as well as their coherent superposition (solid red), for the case in (b).

spatially separated from one another, the outermost pertaining to TPDI by the pump pulse solely and the innermost to one-photon fragmentation of $2s2p$ caused by the probe. Lastly, the lower-right panel displays the energy distribution (logarithmic scale) of the continuum electrons. The outermost energy band matches the excess kinetic energy expected for TPDI of the initial state by the pump pulse, whereas the inner band appears after the action of the probe.

Figure 3(a) displays the conditional angular distributions for electron two provided electron one is ejected at the angles 0° (upper graphs), 45° (center graphs), and 90° (lower graphs) with respect to the laser polarization direction, for the two-color pump-probe scheme described in Fig. 2. Only the coplanar geometry with $\phi_1 = \phi_2 = 0$ is considered. The pump pulse photon energy is chosen to be resonant with the excitation energy of ^3P $2s2p$. Assuming equal energy sharing between the outgoing electrons, they escape with the kinetic energies $E_1 = E_2 = 8.9$ eV (dashed blue) and $E_1 = E_2 = 3.3$ eV (solid red), for the pump and probe pulses, respectively. Nevertheless, the shape of the angular distributions is very similar in both cases, exhibiting two lobes pointing in the backward scattering direction with respect to the escape of electron one. At equal energy sharing, direct back-to-back emission is forbidden in the triplet symmetry [34,45], which is the origin of the node in the angular distributions located at 180° with respect to the direction of emission of electron one.

Figure 3(b) shows the corresponding angular distributions (extracted at equal energy sharing) for a pump pulse of somewhat higher photon energy ($\hbar\omega = 43.3$ eV), which is near resonant with the excitation energy of various DESs in the $^3P^o$ series. Although a nonstationary wave packet comprised of several DESs is launched in this case, the target states are almost degenerate, and as such the relative delay between the pulses plays a minor role in the pump-probe dynamics on the few-femtosecond time scale. The angular distributions of the photoelectrons now turn out to be much more complex than in the $2s2p$ case, made evident by the six-lobe structure revealed in the upper and lower panels. Furthermore, unlike

the angular distributions in Fig. 3(a), the relative magnitude and shape between the pump and probe signals are varying with respect to the ejection angle of electron one.

To explain these findings, we have performed a wave-packet decomposition. Such an analysis reveals that DESs with $A = -1$ in the $n(K,T)N^A$ classification scheme dominate, the most important one being the $3(0,1)2^-$ state comprising more than 85% of the total population in DESs. This is due to the fact that the initial state is of $A = -1$ symmetry and that the approximate propensity rule $\Delta A = 0$ applies to these types of transitions [42]. Accordingly, states with $A = +1$ are significantly less populated in the excitation process, the $3(1,0)2^+$ state being the most important with about 2% population. Nevertheless, it turns out that the $A = +1$ state contributes to the double-ionization yield with an amplitude of the same order of magnitude as the $A = -1$ state. This can be understood from the fact that DESs with $(K,T)^A = (1,0)^+$ tend to have a portion of the wave function located close to the nucleus [42,46], making the double-ionization process more viable. In other words, while some DESs are more easily accessed from the initial state, others may be more easily doubly ionized, and both contributions need to be accounted for.

Following these lines, we show in Fig. 3(c) the characteristic angular distributions of the $3(0,1)2^-$ and $3(1,0)2^+$ states separately, as well as the signal produced from their coherent superposition. The results have been obtained by solving the TDSE for the case of the probe pulse with the relevant DESs as initial states. For comparison reasons, the initial population of each DES is set to its original population size in the wave packet generated by the pump pulse. Analyzing the mixing case, it is found that $3(1,0)2^+$ and $3(0,1)2^-$ are equally important for the double-ionization process and that their mixing gives rise to an interference pattern in the resulting angular distributions. Comparing the solid (red) curves in panels (b) and (c), it is evident that the coherent superposition of $3(1,0)2^+$ and $3(0,1)2^-$ reproduces the full result both in magnitude and shape. This, together with the fact that the distributions of each state individually [dashed (green) and dotted (black) curves in Fig. 3(c)] generally differ from the combined result, merely demonstrate that the six-lobe structure in the parallel and perpendicular geometries occurs due to constructive and destructive interference between the signals from $3(1,0)2^+$ and $3(0,1)2^-$. In contrast, for the case of 45° the combined result is quite similar to the signal from the $3(0,1)2^-$ state only, the interference effect is absent, and $3(1,0)2^+$ contributes very little to the double-ionization dynamics. As such, the relative difference in magnitude between the results in the upper (lower) and middle panels in Fig. 3(b) is partly due to the presence or absence of interference effects. Furthermore, the overall trend that two-color photons produce stronger double-ionization signals than single-color photons, can be attributed to two features: First, the available population in DESs is at a maximum just after the conclusion of the pump pulse, and second, the probe pulse accesses a lower-energy continuum as compared to the pump, i.e., a more dense energy space.

In summary, we have studied the laser-driven two-photon two-electron breakup of the helium ^3S $1s2s$ metastable state. The process has been modeled within a fully *ab initio* numerical framework. We observe a highly nonlinear response with respect to the duration of the applied laser pulse when the driving frequency of the field is resonant with intermediate DESs. The underlying REMPI process is expected to play a major role in double-ionization processes in general, and in particular for cases where the ionizing electrons originate from different orbitals. A pump-probe scheme is proposed to investigate the role of intermediate DESs in the double-ionization dynamics. In the present pump-probe protocol, the driving frequency of the pump pulse is tuned to different resonant transitions between the initial state and the DESs in the $^3P^o$ series. We observe that while some intermediate DESs are easily accessed from the initial state, others are more easily doubly ionized due to their angular and radial correlation properties. Fundamental differences in terms of shape and yield of the corresponding angular distributions are revealed, depending on the characteristics of the DESs. More importantly, it is found that the interplay between the different intermediate channels gives rise to interferences in the double-ionization dynamics, which are clearly expressed in the correlated angular distributions of the emitted photoelectrons. As such, the correlated properties of the DESs are vital in order to describe the full breakup of the ^3S $1s2s$ state. As an outlook, it would be interesting to perform a study of the interference dynamics on a longer time scale, in order to explore to what extent and how the autoionization nature of the DESs influences the process.

This work was supported by the Bergen Research Foundation, the Norwegian Metacenter for Computational Science (Notur), the European COST Action CM1204 (XLIC), and the program AURORA [Norges Forskningsråd (NFR) for Norway and ministères des Affaires étrangères (MAE) et de l´Enseignement supérieur et de la Recherche (MESR) for France]. All calculations were performed on the Cray XE6 (Hexagon) supercomputer installation at Parallab, University of Bergen (Norway). The authors thank Eva Lindroth for useful discussions on the topic of doubly excited states and for sending results in electronic form.

[1] J. Colgan and M. S. Pindzola, Phys. Rev. Lett. **88**, 173002 (2002).

[2] S. Laulan and H. Bachau, Phys. Rev. A **68**, 013409 (2003).

[3] B. Piraux, J. Bauer, S. Laulan, and H. Bachau, Eur. Phys. J. D **26**, 7 (2003).

[4] E. Foumouo, G. L. Kamta, G. Edah, and B. Piraux, Phys. Rev. A **74**, 063409 (2006).

[5] R. Shakeshaft, Phys. Rev. A **76**, 063405 (2007).

[6] D. A. Horner, F. Morales, T. N. Rescigno, F. Martín, and C. W. McCurdy, Phys. Rev. A **76**, 030701(R) (2007).

[7] L. A. A. Nikolopoulos and P. Lambropoulos, J. Phys. B **40**, 1347 (2007).

[8] J. Feist, S. Nagele, R. Pazourek, E. Persson, B. I. Schneider, L. A. Collins, and J. Burgdörfer, Phys. Rev. A **77**, 043420 (2008).

[9] X. Guan, K. Bartschat, and B. I. Schneider, Phys. Rev. A **77**, 043421 (2008).

[10] X. Guan, O. Zatsarinny, C. J. Noble, K. Bartschat, and B. I. Schneider, J. Phys. B **42**, 134015 (2009).
[11] R. Nepstad, T. Birkeland, and M. Førre, Phys. Rev. A **81**, 063402 (2010).
[12] M. Førre, S. Selstø, and R. Nepstad, Phys. Rev. Lett. **105**, 163001 (2010).
[13] A. Palacios, T. N. Rescigno, and C. W. McCurdy, Phys. Rev. A **79**, 033402 (2009).
[14] A. Palacios, D. A. Horner, T. N. Rescigno, and C. W. McCurdy, J. Phys. B **43**, 194003 (2010).
[15] H. Bachau, Phys. Rev. A **83**, 033403 (2011).
[16] H. Hasegawa, E. J. Takahashi, Y. Nabekawa, K. L. Ishikawa, and K. Midorikawa, Phys. Rev. A **71**, 023407 (2005).
[17] Y. Nabekawa, H. Hasegawa, E. J. Takahashi, and K. Midorikawa, Phys. Rev. Lett. **94**, 043001 (2005).
[18] P. Antoine, E. Foumouo, B. Piraux, T. Shimizu, H. Hasegawa, Y. Nabekawa, and K. Midorikawa, Phys. Rev. A **78**, 023415 (2008).
[19] A. A. Sorokin, M. Wellhöfer, S. V. Bobashev, K. Tiedtke, and M. Richter, Phys. Rev. A **75**, 051402(R) (2007).
[20] A. Rudenko, L. Foucar, M. Kurka, T. Ergler, K. U. Kühnel, Y. H. Jiang, A. Voitkiv, B. Najjari, A. Kheifets, S. Lüdemann *et al.*, Phys. Rev. Lett. **101**, 073003 (2008).
[21] M. Kurka, J. Feist, D. A. Horner, A. Rudenko, Y. H. Jiang, K. U. Kühnel, L. Foucar, T. N. Rescigno, C. W. McCurdy, R. Pazourek *et al.*, New J. Phys. **12**, 073035 (2010).
[22] J. Colgan, M. S. Pindzola, and F. Robicheaux, J. Phys. B **41**, 121002 (2008).
[23] F. Morales, F. Martín, D. A. Horner, T. N. Rescigno, and C. W. McCurdy, J. Phys. B **42**, 134013 (2009).
[24] X. Guan, K. Bartschat, and B. I. Schneider, Phys. Rev. A **82**, 041404(R) (2010).
[25] X. Guan, K. Bartschat, and B. I. Schneider, Phys. Rev. A **84**, 033403 (2011).
[26] A. S. Simonsen, S. A. Sørngård, R. Nepstad, and M. Førre, Phys. Rev. A **85**, 063404 (2012).
[27] I. A. Ivanov and A. S. Kheifets, Phys. Rev. A **87**, 023414 (2013).
[28] R. Nepstad and M. Førre, Phys. Rev. A **84**, 021402(R) (2011).
[29] Z. J. Teng and R. Shakeshaft, Phys. Rev. A **49**, 3597 (1994).
[30] H. W. van der Hart, K. W. Meyer, and C. H. Greene, Phys. Rev. A **57**, 3641 (1998).
[31] J. Colgan and M. S. Pindzola, Phys. Rev. A **67**, 012711 (2003).
[32] A. Emmanouilidou, T. Schneider, and J.-M. Rost, J. Phys. B **36**, 2717 (2003).
[33] K. Stefańska, F. Reynal, and H. Bachau, Phys. Rev. A **85**, 053405 (2012).
[34] G. S. J. Armstrong and J. Colgan, Phys. Rev. A **86**, 023407 (2012).
[35] M. Schuricke, G. Veeravalli, G. Zhu, C. Dornes, K. Joachimsmeyer, A. Dorn, and J. Ullrich, J. Phys. Conf. Ser. **388**, 032054 (2012).
[36] A. Czasch, M. Schöffler, M. Hattass, S. Schössler, T. Jahnke, T. Weber, A. Staudte, J. Titze, C. Wimmer, S. Kammer *et al.*, Phys. Rev. Lett. **95**, 243003 (2005).
[37] T. Morishita, S. Watanabe, and C. D. Lin, Phys. Rev. Lett. **98**, 083003 (2007).
[38] A. Hishikawa, M. Fushitani, Y. Hikosaka, A. Matsuda, C.-N. Liu, T. Morishita, E. Shigemasa, M. Nagasono, K. Tono, T. Togashi *et al.*, Phys. Rev. Lett. **107**, 243003 (2011).
[39] J. Feist, S. Nagele, C. Ticknor, B. I. Schneider, L. A. Collins, and J. Burgdörfer, Phys. Rev. Lett. **107**, 093005 (2011).
[40] H. Bachau, E. Cormier, P. Decleva, J. E. Hansen, and F. Martín, Rep. Prog. Phys. **64**, 1815 (2001).
[41] C. de Boor, *A Practical Guide to Splines*, revised ed. (Springer-Verlag, New York, 2001).
[42] C. D. Lin, Phys. Rev. A **29**, 1019 (1984).
[43] C. D. Lin, Phys. Rev. Lett. **51**, 1348 (1983).
[44] E. Lindroth, Phys. Rev. A **49**, 4473 (1994).
[45] F. Maulbetsch and J. S. Briggs, J. Phys. B **28**, 551 (1995).
[46] M. Cortés, A. Macías, F. Martín, and A. Riera, J. Phys. B **26**, 3269 (1993).